Eleventh South African Conference on Computational and Applied Mechanics
SACAM 2018
Vanderbijlpark, South Africa, 17-19 September 2018

A probabilistic quarter-car model for predicting worst-case vehicle performance

Anria Clarke[a], Deon Sabatta[b]

[a]*Defence, Peace, Safety and Security – Landward Sciences, CSIR. PO Box 395, Pretoria 0001, South Africa.*

[b]*Department of Electrical and Electronic Engineering Science, Faculty of Engineering and the Built Environment, University of Johannesburg. PO Box 524, Johannesburg 2006, South Africa.*

email address : aclarke@csir.co.za[a], dsabatta@uj.ac.za[b]

Abstract

Vehicle preview models have gained increasing popularity in recent years as a means of predicting potentially hazardous vehicle control inputs and attempting to mitigate their effects. These models are even more important in the field of autonomous vehicles as the vehicle itself is providing the potentially hazardous control input. In these cases, it is important to verify that these inputs will actually achieve the desired control objectives, and not result in a loss of traction or destabilisation of the vehicle.

Unfortunately, the validity of these models is limited by the fidelity of the mathematical model and the accuracy of the estimated vehicle parameters. In the real-world, vehicle parameters are subject to change over time as a result of wear-and-tear, installation of after-market parts and vehicle loading.

In this paper a method for propagating any uncertainty in the vehicle parameters through these models to determine variability in the output is presented. In doing so, worst-case estimates of the performance of the vehicle in certain situations may be provided.

The authors introduce this method using the basic quarter-car model as a demonstrator. After developing the statistical model, the estimated outputs are verified using a Monte Carlo simulation, and conclusions are drawn on the performance of the vehicle under parameter uncertainty.

The results show that under ideal road conditions, any parameter uncertainty has very little effect on the road-holding performance of a vehicle, but on increasingly rougher roads, this parameter uncertainty plays a substantially larger role. As such, the methods presented in this paper are therefore suitable for use in self-driving cars that are designed to operate in off-road conditions.

Keywords: Quarter-car model; stochastic mechanics; autonomous vehicle; dynamic load coefficient

1. Introduction

Vehicle preview models are gaining increasing use in the field of vehicle dynamics and safety to predict and help prevent potentially hazardous situations [1]–[3]. These models attempt to predict the results of actions taken by the driver, and based on these predictions, controllable vehicle systems alter the dynamic response of the vehicle in order to prevent or reduce the likelihood of undesirable outcomes (e.g. roll-over).

Preview models are of even more importance in autonomous vehicles as it is the autonomous vehicle itself that is providing the potentially unsafe input. In this case, a vehicle preview model would be used to ensure that the desired actions lead to the expected result, rather than trying to predict the result of unknown inputs.

The effectiveness of these preview models is directly linked to the accuracy of the mathematical model and the extent to which the model and associated vehicle parameters represent the true vehicle. As these vehicles are used outside the control of the manufacturer, variations of these model parameters can be attributed to factors such as component wear, the fitment of after-market parts, tyre inflation and wear, as well as changes in vehicle payload [4], [5].

To account for this, one may either attempt to predict the vehicle parameters in real-time by matching simulated results to measurements, or alternatively, develop more complex models that can handle any potential variation in these parameters statistically. This paper follows the second approach by adapting a quarter-car model with random road profile input, and propagating any potential uncertainty in the vehicle parameters through to the output predictions to obtain worst-case estimates of the predicted values.

The need for these statistical models arises as part of the CSIR GBAT Autonomous Vehicle project. Unlike most autonomous or semi-autonomous vehicles such as the Google car or Tesla's range of self-driving cars, the GBAT vehicle (shown in Fig. 1) is being designed to operate at relatively high-speeds (>40km/h and <80km/h) in both off-road and unstructured environments. We will show that in these environments, the effect of parameter uncertainty on road-holding is much more pronounced than on smooth roads, justifying the need for the statistical analysis. The models we present relate to what is known as the reflexive driver component of the autonomous vehicle control system whose goal it is to predict potentially unsafe maneuvers and take corrective action before it occurs.

When it comes to the choice of vehicle model, many options exist from the simple quarter-car model [6], to half-car, full-car [7], roll-and-yaw models [8], etc. The choice of model is generally influenced by the intended application. For this paper, we have used the most basic model available as a demonstration of the method to propagate parameter uncertainty through the model to the output parameters. As a result, we are only able to make first-order estimates on the road holding ability of the vehicle.

Previous work on passing parameter uncertainty through vehicle models has mostly focused on the design aspects [9] where the designer can choose the vehicle parameters to optimise metrics such as ride comfort, suspension working space and road holding. Other work in [5] also looks at the effects of parameter uncertainty on vehicle models, but in this case from a vibrations stand-point, analysing the mode shapes and frequencies.

Fig. 1. Autonomous vehicle platform.

From here we proceed to introduce the linear quarter-car model and some metrics to evaluate road holding and cornering in Section 2. Sections 3 and 4 introduce the statistical methods used to account for unknown road surfaces and their effect on the metrics introduced in Section 2. Section 5 covers the primary contribution of the paper where the Unscented Transform is used to propagate the effects of uncertain vehicle parameters onto the road holding metrics. We then validate the performance of the proposed method using Monte Carlo simulations for various configurations of uncertainty in the vehicle parameters in Section 6. Finally, Section 7 presents a few results showing the stability boundaries of the vehicle on various road surfaces for both straight and curved paths as predicted by the proposed method. The paper ends with the conclusions and future work in Section 8.

2. Vehicle model

Two vehicle models have been adopted for this work: a linear quarter-car model (discussed in Section 2.1), and a simplified cornering model (discussed in Section 2.2).

2.1. Quarter-car model

Quarter-car models, shown in Fig. 2, are widely used in vehicle response studies to predict vertical acceleration of the vehicle body which is linked to ride comfort, and road-holding which, in turn, is linked to vehicle drive safety [6], [7]. The model describes the vertical motion of the vehicle body and wheel at one corner of a vehicle, and is excited by a road surface displacement input as a function of time. The equations of motion of the model are provided in (1) and (2).

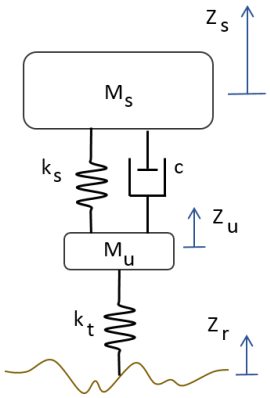

Fig. 2. Representation of quarter-car model.

In the equations below (also refer to Fig. 2), the mass of the vehicle body (also known as the sprung mass) is denoted by M_s, and the mass of the wheel and some of the suspension components (lumped together and referred to as the unsprung mass) is denoted by M_u. Vertical acceleration, $\ddot{Z}$, velocity, $\dot{Z}$, and displacement, Z, of the sprung- and unsprung masses are denoted by Z_s and Z_u respectively. The suspension spring stiffness and damping are denoted by k_s and c, while the tyre stiffness is denoted by k_t. Tyre damping is considered to be negligible. The vertical displacement of the road surface is denoted by Z_r.

$$M_s\ddot{Z}_s = -k_s(Z_s - Z_u) - c\left(\dot{Z}_s - \dot{Z}_u\right) \tag{1}$$

$$M_u\ddot{Z}_u = k_s(Z_s - Z_u) + c\left(\dot{Z}_s - \dot{Z}_u\right) - k_t(Z_u - Z_r) \tag{2}$$

The response outputs of interest from the quarter-car model are [9]–[12]:

i. Vertical acceleration of the vehicle body ($\ddot{Z}_s$) which is used to quantify the ride comfort experienced by the passengers;

ii. Suspension travel ($Z_s - Z_u$) which is used to determine the necessary work (rattle) space or packaging requirements of the suspension design; and

iii. Vertical tyre force ($F_{tz} = k_t(Z_u - Z_r)$) which gives an indication of road-holding and thus the handling capability.

The road holding metric applicable to the quarter-car model that we will consider is that of the Dynamic Load Coefficient (DLC) as presented in [13]. While the statistical distributions of the three metrics in i-iii above may be evaluated, a more useful interpretation of the measurements related to vertical tyre force in practice is the DLC which is related to the likelihood of loss of ground contact. The DLC is the standard deviation of the tyre vertical force, $\sigma_{F_{tz}}$, normalised with respect to the static tyre force, $F_{tz,static}$, as shown in (3). In other words, the DLC expresses the degree to which the tyre normal force is expected to vary as a percentage of the static force. Múčka [13] cites typical values of DLC in the range of 0.1 to 0.15 and upper safety limits of 0.3. Statistically, a DLC of 0.3 relates to a 0.043% chance of the tyre normal force dropping below 0N (loss of ground contact) or equivalently, a 1% chance of the tyre normal force dropping below about 30% of its static value.

$$DLC = \frac{\sigma_{F_{tz}}}{F_{tz,static}} \tag{3}$$

In (3) the static tyre force may be taken as $F_{tz,static} = g(M_s + M_u)$, where g is the gravitational acceleration constant.

2.2. Cornering model

In order to evaluate vehicle handling during cornering, a simplified cornering model is adopted. This cornering model is based on the steady-state cornering of a bicycle model presented in [14]. The results using this model are therefore approximate, and a more detailed model including vehicle roll would have to be considered for more accurate predictions. In addition, we assume that the driving algorithm will automatically set the slip angle to the maximum possible value to achieve the desired lateral force.

In [14], it is shown that the lateral force produced by each wheel in the bicycle model is proportional to the vehicle load on that wheel. This allows us to extend the quarter car model to determine the lateral force produced by a tyre, F_{ty}, as,

$$F_{ty} = \frac{(M_s + M_u)v^2}{RoC} \tag{4}$$

Where M_s and M_u are the sprung and unsprung masses for the model, v is the forward velocity and *RoC* is the radius of curvature of the turn.

Once we have the lateral force required to be produced by the tyre, we can estimate the minimum vertical tyre force $F_{tz,min}$ using a tyre model at maximum slip angle before tyre saturation occurs. When calculating the DLC, we then normalise by $(F_{tz,static} - F_{tz,min})$, thereby taking into account this minimum required vertical force. This essentially rescales the DLC from a straight-road approximation to a cornering model.

3. Statistical analysis

Given the differential equations of the previous section, we can define transfer functions in the Laplace domain between the road input $Z_r(s)$ and position of the sprung-, $Z_s(s)$, and unsprung-mass, $Z_u(s)$. The response outputs of interest (refer to i-iii in Section 2.1) can then be defined in terms of these parameters as follows.

$$\ddot{Z}_s(s) = s^2 Z_s(s) \tag{5}$$

$$Z_{ws}(s) = Z_s(s) - Z_u(s) \tag{6}$$

$$F_{tz}(s) = k_t(Z_u(s) - Z_r(s)) \tag{7}$$

If we assume that the road input is a zero-mean wide-sense stationary random process with Power Spectral Density (PSD), $S_r(\omega)$, we can determine the PSD of the random processes associated with each of the output functions defined above as [15],

$$S_X(\omega) = |H_X(j\omega)|^2 S_r(\omega) \quad (8)$$

Where $H_X(j\omega)$ is the frequency domain transfer function between the input $Z_r(s)$ and output ($\ddot{Z}_s$, Z_{ws}, orF_{tz}) obtained through the substitution of $s = j\omega$ into equations (5) – (7) above.

Once we have the output PSD, we can recover the autocorrelation function of the output random processes as the inverse Fourier transform of the PSD,

$$R_X(\tau) = \int_{-\infty}^{\infty} S_X(\omega) e^{j\omega\tau}\, d\omega \quad (9)$$

Since we assumed that the input random process is zero-mean, we can find the variance of the output parameters as,

$$\sigma_X^2 = E[X^2] - E[X]^2 = R_X(0) = \int_{-\infty}^{\infty} S_X(\omega) d\omega \quad (10)$$

While closed form integrals for this expression exist in certain cases (cf [9]), we advocate the use of numerical integration when evaluating this expression for the following reasons:

i. Numerical integration permits a wider range of input PSD functions and the use of more complex models where the closed-form solutions are no longer tractable.

ii. The PSD $S_X(\omega)$ is an even function of ω, (i.e. $S_X(\omega) = S_X(-\omega)$) which reduces the evaluation interval.

iii. Since both the input PSD and the transfer function tend to zero rapidly as ω approaches infinity, this further reduces the practical evaluation interval.

iv. Numerical evaluation of the integrals allows for frequency weighted computation of certain parameters such as ride-comfort according to BS6841 [16].

We are now able to predict the variance of the output parameters given known vehicle parameters and the PSD of the road input.

4. Road surface PSD

The literature provides many approximations of the PSD for typical road surfaces [17]. The primary source of this information is ISO8608 [18] which advocates the use of a PSD function of the form

$$S_r(\omega) = \frac{A_b v}{\omega^2} \quad (11)$$

Where A_b is related to the road class as defined in the Standard and v is the vehicle velocity. The problem with this PSD is that it tends to overestimate the variability of the road surface at low frequencies since $\lim_{\omega \to 0} S_r(\omega) \to \infty$.

To overcome this, [9] recommends the use of the "two-slope" PSD given by,

$$S_r(\omega) = \frac{A_v s_c}{s_c^2 + \omega^2} \quad (12)$$

Where $s_c = av$ and a relates to the maximum variability of the road surface. The parameters for this PSD related to each of the ISO8608 road classes are provided in Table 1.

5. Incorporating the effects of uncertain vehicle parameters

Using the methods of the previous section, we can predict the desired output parameters given an uncertain road profile. We now consider how to incorporate uncertainties in the vehicle parameters on these outputs. While the differential equations are linear in the outputs, they are non-linear in the parameters. We therefore need a method of propagating any parameter uncertainty through this non-linear model.

Table 1. PSD parameters of various road classes.

Road Class	A_v [m^2]
A	15.86x10^{-6}
B	63.42x10^{-6}
C	253.7x10^{-6}
D	1.015x10^{-3}
E	4.059x10^{-3}
$a = 0.4$ rad/m (see [9])	

Typically, this is achieved by linearising the transform around the mean and propagating the uncertainty through this linearised transform. In this case, Gaussian distributed uncertainty is a good choice as the Gaussian random variables remain Gaussian through linear transforms. The choice of Gaussian distributed uncertainty is also motivated by the Central Limit Theorem [15].

As we do not have a direct transform between the input and output variables of interest, a linear transform will have to be approximated through multiple samples and numerical derivatives. In [19], Julier et al. offer an alternative called the Unscented Transform. The rationale behind this approach is to approximate the uncertain distribution (which we have assumed to be Gaussian) rather than the non-linear transform which is more exact. The Unscented Transform approximates the input distribution by a collection of points known as sigma-points which are then transformed through the non-linear system and the statistics are recomputed on the transformed points.

The choice of these sigma points is still an open problem, and many proposals have been made with various strengths and weaknesses. A detailed review of some of these is available in [20].

From the previous sections, we have a statistical model that predicts the mean and variance of an output parameter given known vehicle parameters (constants in the ODEs (1) and (2)). For simplicity, we represent this process as a transform between these vehicle parameters and the desired output statistics. Since in this paper we are only interested in the DLC (note the minimum RoC is computed using the DLC), we can represent this transform as,

$$DLC = T(M_s, M_u, k_s, c, k_t) \tag{13}$$

For fixed values of the vehicle parameters, this transform yields a constant for the DLC; however, if we replace the vehicle parameters with stochastic variables then the DLC will itself become a stochastic variable.

To determine the mean and variance of the DLC under uncertainty in the vehicle parameters we make use of the Unscented Transform. To do this, we first represent the vehicle parameters as an n-dimensional multivariate Gaussian random variable with mean μ and covariance Σ. In this manner, we can include high-level relationships between parameters as off-diagonal elements in the covariance matrix, as well as representing constant terms by setting the covariance elements to zero.

We can then find the $2n$ symmetric sigma-points s_i as proposed in [21] as

$$s_i = \begin{cases} \left[\sqrt{n\Sigma}\right]_i + \mu, & i = 1..n \\ \left[-\sqrt{n\Sigma}\right]_{(i-n)} + \mu, & i = (n+1)..2n \end{cases} \tag{14}$$

where the subscript notation $[A]_i$ represents the i-th column of the matrix A.

These sigma points represent sets of vehicle parameters at which the original transform should be evaluated to determine the mean and variance of the output variable. To determine the mean and variance of the DLC, we compute the population mean and variance of all the transformed sigma-points as,

$$\mu_{DLC} = \frac{1}{n}\sum_{i=1}^{n} T(s_i) \qquad \sigma_{DLC}^2 = \frac{1}{n}\sum_{i=1}^{n} (T(s_i) - \mu_{DLC})^2 \tag{15}$$

6. Simulation

In order to verify the ability of the statistical method to predict road-holding a Monte Carlo simulation is performed using MATLAB® software. To account for uncertainty in vehicle parameters they are generated randomly to follow a normal distribution with mean (midpoint between selected minimum and maximum values) and standard deviation listed in Table 2. The standard deviation is selected to produce 95% of the generated vehicle parameters between specified maximum and minimum values, using

$$\sigma = \frac{Maximum - Minimum}{4} \tag{16}$$

Table 2. Variation in uncertain vehicle parameters.

Parameter	Maximum	Minimum	Mean	Standard Deviation
Sprung Mass [kg]	675	430	552.5	61.25
Unsprung Mass [kg]	66.3	44.2	55.25	5.525
Suspension Stiffness [N/m]	50 x10^3	20 x10^3	35 x10^3	7.5 x10^3
Damping [Ns/m]	10 x10^3	3 x10^3	6.5 x10^3 (5 x10^3)	1.75 x10^3
Tyre Stiffness [N/m]	180 x10^3	60 x10^3	120 x10^3 (160 x10^3)	30 x10^3

To generate the random road profiles for the Monte Carlo simulations, we model the road as a zero-mean Gaussian random process with autocorrelation function $R_r(\tau)$ which is found as the inverse Fourier transform of the road PSD $S_r(\omega)$. A class B road is used, with $A_v = 63.42 \times 10^{-6}$ (refer to Table 1). The vehicle travel speed is $v = 20m/s$, and the duration of excitation is 15s, resulting in a road length of 300m.

For the first set of simulations one vehicle parameter is generated randomly while the others are set equal to the mean (refer to Table 2), except for the damping of the suspension and the tyre stiffness for which the values given in brackets are used. For each varied parameter 10 000 iterations are performed. Thereafter the mean and variance of the resulting distribution of DLC of each simulation set is established. Monte Carlo simulation results are compared to results from the proposed method in Table 3. The solving time of the Monte Carlo simulation is just under 3 hours for 10 000 iterations, while the statistical method takes between 2 to 3 seconds to generate the same results.

From Table 3 it may be deduced that the proposed method accurately predicts the tyre force standard deviation for variations in sprung mass, damping and tyre stiffness. The standard deviation for varying unsprung mass and suspension stiffness from the Monte Carlo simulation is much higher than predicted by the proposed method. The cause of the discrepancy was found to be the presence of numerical error in the Monte Carlo simulation results. An additional Monte Carlo simulation was performed for constant vehicle parameters. The results are shown in Table 3, in the row labeled “None”. The analytical solutions for varied spring stiffness and suspension damping, as well as constant vehicle parameters, are also compared to the Monte Carlo simulation results in Fig. 3. The results from the two methods for varying damping correlate well, while the effect of uncertainty in suspension stiffness is overshadowed by the numerical error resulting from the numerical integration process of the ordinary differential equation solver.

For the next set of simulations all vehicle parameters were generated randomly as described before. The same road surface excitation used in previous simulation sets is used in this set (class B road and vehicle speed of 20m/s). The Monte Carlo simulation consisted of 50 000 iterations. The mean and standard deviation of the resulting distribution of tyre force standard deviation is compared to the proposed method in Table 3, in the row labeled “All”. The normal

distributions of the varied vehicle parameters and the distribution of tyre force standard deviation are shown in Fig. 4, where it may be seen that the results from the two methods correlate well.

Table 3. Normal distribution of DLC.

	Unscented Transform		Monte Carlo Simulation	
Varied Parameter	Mean	Standard Deviation	Mean	Standard Deviation
Sprung Mass	0.1656	0.0206	0.1668	0.0196
Unsprung Mass	0.1634	0.0009	0.1646	0.0055
Suspension Stiffness	0.1639	0.0020	0.1650	0.0057
Damping	0.1759	0.0157	0.1783	0.0163
Tyre Stiffness	0.1353	0.0205	0.1364	0.0223
None	0.1622	0	0.1647	0.0054
All	0.1495	0.0318	0.1507	0.0332

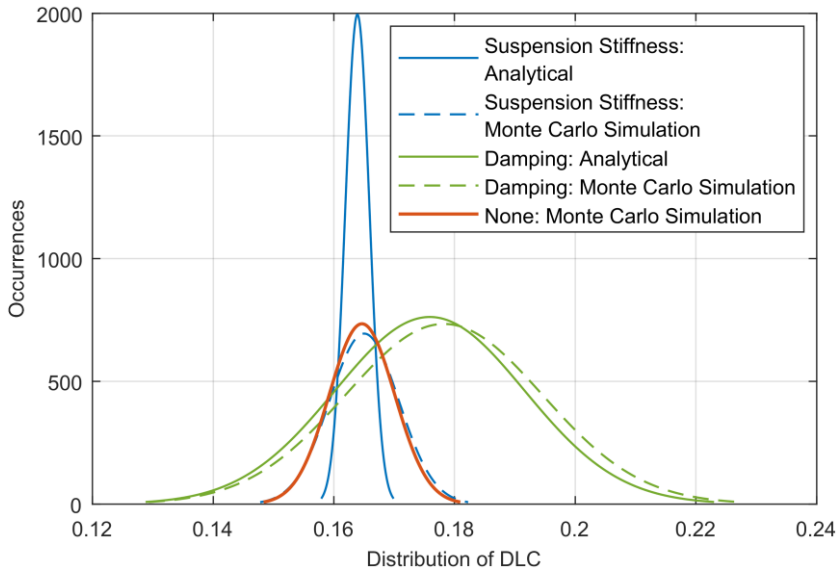

Fig. 3. DLC resulting from numerical error ("None") compared to other results sets.

7. Results

In this section, we present some theoretical results of the statistical model as applicable to road-holding for the autonomous vehicle. We will consider two metrics, the first being the DLC (discussed in Section 2.1) and the second the minimum RoC from the simplified cornering model (discussed in Section 2.2). Based on the typical values of [13], a DLC of 0.3 has been adopted as the safety threshold in this work.

Fig. 5 and Fig. 6 present the DLC values for the nominal and statistical models for class B and C roads respectively. The shaded region represents the 2-sigma bounds of the statistical model, and the nominal model corresponds to the solution for no uncertainty in the vehicle parameters. From these graphs, we can see that for the case of a class B road, even in the presence of substantial uncertainty in the vehicle parameters, the vehicle DLC remains below the 0.3 safety threshold for all speeds up to 20m/s. In the case of a class C road, the parameter uncertainty reduced the safe travel speed from around 8.3m/s to 4.8m/s – a 42% reduction in safe travel speed.

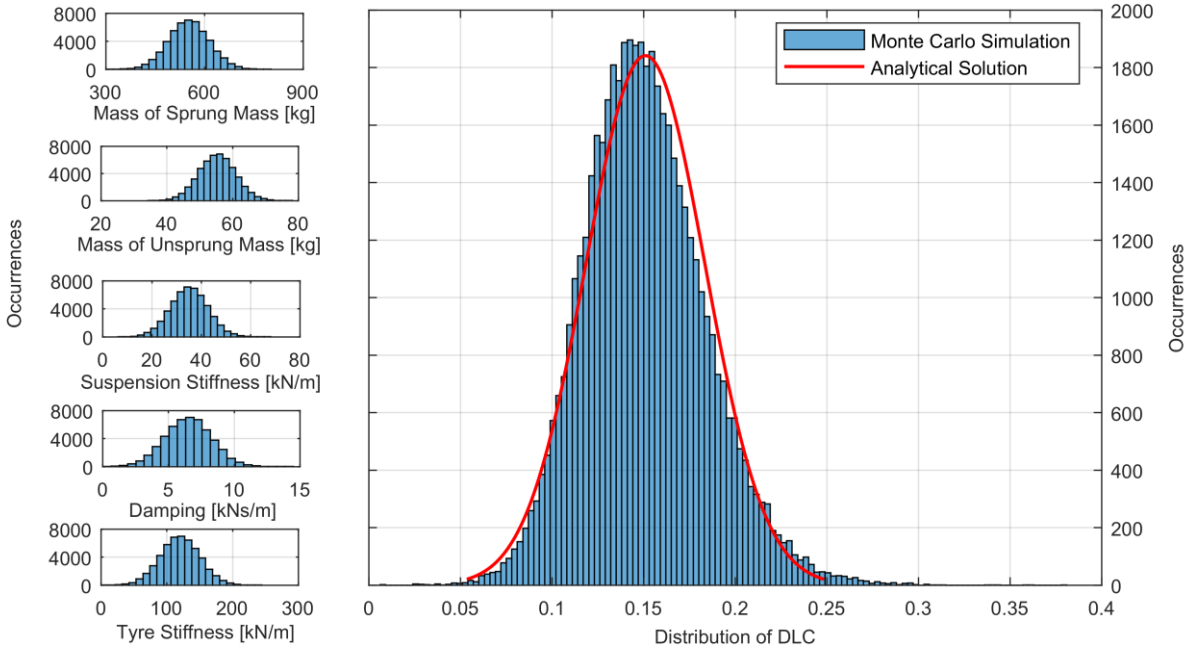

Fig. 4. Effect of vehicle parameter uncertainty (left) on the DLC (right).

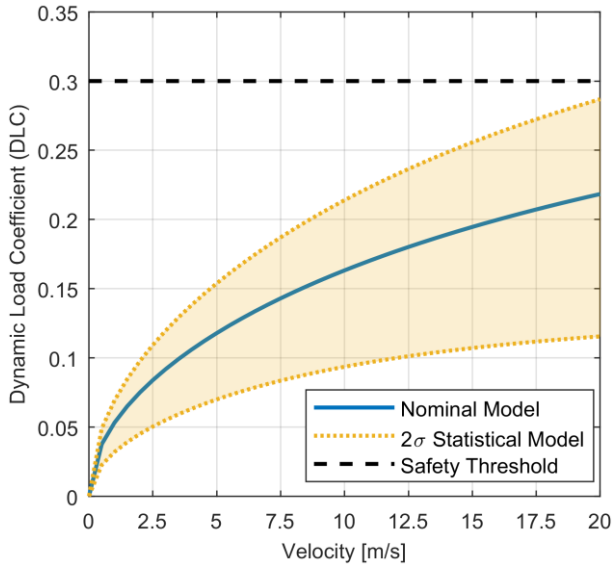

Fig. 5. DLC vs. velocity for a class B road.

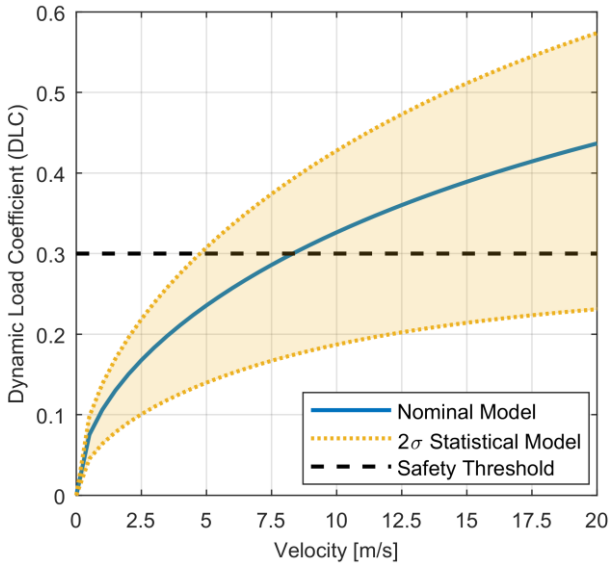

Fig. 6. DLC vs. velocity for a class C road.

When working with the cornering model presented in Section 2.2, the method requires the overall mass of the components supported by the suspension system (M_s and M_u). However, in our case, these parameters are not known as a result of the uncertainty in the vehicle parameters. This issue is however handled elegantly by the proposed Unscented Transform method, as it evaluates the model at each of the sigma-points, where the masses above are explicitly specified, thereby automatically including the uncertainty in M_s and M_u into the cornering model.

Fig. 7 and Fig. 8 show the minimum safe RoC for class B and C roads at different speeds. Since the cornering model used to create these graphs provides the DLC as a function of RoC, we used a gradient-based solving algorithm to find the RoC for which the DLC was equal to 0.3 (the proposed worst-case safety threshold).

Since cornering essentially increases the required minimum normal force, we can see in these figures how the minimum safe RoC approaches infinity as the DLC for straight motion approaches the 0.3 threshold. Once again we note that the effects of parameter uncertainty are far more pronounced for uneven road surfaces.

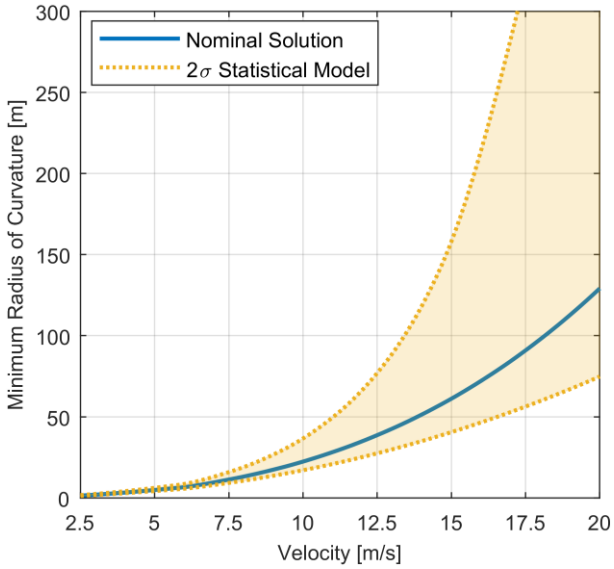

Fig. 7. Minimum safe RoC before loss of traction on class B roads.

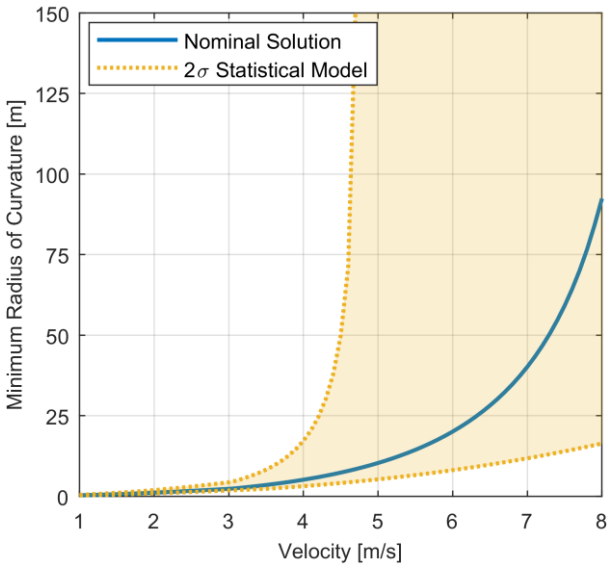

Fig. 8. Minimum safe RoC before loss of traction on class C roads.

8. Conclusion

In this paper, we have presented a stochastic quarter-car model subject to random road input together with a method of propagating parameter uncertainty in the model through to the output variables. We have verified the performance of the algorithm through the use of a Monte Carlo simulation and demonstrated that the proposed method provides a reasonable approximation of the true distributions, despite the inherent non-linear relationship between the vehicle parameters and the output measurements.

The proposed method allows us to determine the worst-case performance of the vehicle under various conditions and parameter uncertainty. We have shown that the difference between this worst-case performance and nominal models increases as the quality of the road surface decreases, making this analysis of particular interest for off-road vehicles.

In future work, we are looking at extending these methods to more detailed models to include effects such as roll and pitch dynamics. Two open problems that we have not yet addressed are the extent to which DLC predicts handling and how to estimate the PSD of the road surface in real-time so that we can apply the appropriate preview model.

References

[1] S. Yim, “Design of a preview controller for vehicle rollover prevention,” *IEEE Transactions on Vehicular Technology*, vol. 60, no. 9, pp. 4217–4226, 2011.

[2] Y. Yoon, J. Shin, H. J. Kim, Y. Park, and S. Sastry, “Model-predictive active steering and obstacle avoidance for autonomous ground vehicles,” *Control Engineering Practice*, vol. 17, no. 7, pp. 741–750, 2009.

[3] A. Y. Ungoren and H. Peng, “An adaptive lateral preview driver model,” *Vehicle system dynamics*, vol. 43, no. 4, pp. 245–259, 2005.

[4] M. Gobbi, F. Levi, and G. Mastinu, “Multi-objective stochastic optimisation of the suspension system of road vehicles,” *Journal of sound and vibration*, vol. 298, no. 4–5, pp. 1055–1072, 2006.

[5] W. Gao, N. Zhang, and J. Dai, “A stochastic quarter-car model for dynamic analysis of vehicles with uncertain parameters,” *Vehicle System Dynamics*, vol. 46, no. 12, pp. 1159–1169, 2008.

[6] D. Fischer and R. Isermann, “Mechatronic semi-active and active vehicle suspensions,” *Control engineering practice*, vol. 12, no. 11, pp. 1353–1367, 2004.

[7] S. M. Savaresi, C. Poussot-Vassal, C. Spelta, O. Sename, and L. Dugard, *Semi-active suspension control design for vehicles*. Elsevier, 2010.

[8] M. Abe, *Vehicle handling dynamics: theory and application*. Butterworth-Heinemann, 2015.

[9] M. Gobbi and G. Mastinu, “Analytical description and optimization of the dynamic behaviour of passively

suspended road vehicles," *Journal of sound and vibration*, vol. 245, no. 3, pp. 457–481, 2001.
[10] D. Cao, X. Song, and M. Ahmadian, "Editors' perspectives: road vehicle suspension design, dynamics, and control," *Vehicle system dynamics*, vol. 49, no. 1–2, pp. 3–28, 2011.
[11] D. E. Ivers and L. R. Miller, "Experimental comparison of passive, semi-active on/off, and semi-active continuous suspensions," SAE Technical Paper, 1989.
[12] G. Verros, S. Natsiavas, and C. Papadimitriou, "Design optimization of quarter-car models with passive and semi-active suspensions under random road excitation," *Modal Analysis*, vol. 11, no. 5, pp. 581–606, 2005.
[13] P. Múčka, "Simulated Road Profiles According to ISO8608 in Vibration Analysis," *Journal of Testing and Evaluation*, vol. 46, no. 1, pp. 1–14, 2017.
[14] T. D. Gillespie, *Fundamentals of Vehicle Dynamics.* Warrendale, PA: Society of Automotive Engineers, Inc, 1992.
[15] A. Leon-Garcia, *Probability and Random Processes for Electrical Engineering*. Addison-Wesley, 1994.
[16] *British Standard Guide to measurement and evaluation of human exposure to whole-body mechanical vibration and repeated shock, BS6841*. British Standards Institution, 1987.
[17] C. Dodds and J. Robson, "The description of road surface roughness," *Journal of sound and vibration*, vol. 31, no. 2, pp. 175–183, 1973.
[18] *Mechanical vibration - Road surface profiles - Reporting of measured data, ISO8608*. The International Organization for Standardization (ISO), Geneva, 1995.
[19] S. Julier, J. Uhlmann, and H. F. Durrant-Whyte, "A new method for the nonlinear transformation of means and covariances in filters and estimators," *IEEE Transactions on automatic control*, vol. 45, no. 3, pp. 477–482, 2000.
[20] H. M. Menegaz, J. Y. Ishihara, G. A. Borges, and A. N. Vargas, "A systematization of the unscented Kalman filter theory," *IEEE Transactions on automatic control*, vol. 60, no. 10, pp. 2583–2598, 2015.
[21] J. K. Uhlmann, "Dynamic map building and localization: New theoretical foundations," PhD Thesis, University of Oxford, Oxford, 1995.